

## Crystal-field excitations in $\text{Nd}_2\text{CuO}_4$ , $\text{Pr}_2\text{CuO}_4$ , and related $n$ -type superconductors

A. T. Boothroyd,\* S. M. Doyle, and D. M<sup>c</sup>K. Paul

*Department of Physics, University of Warwick, Coventry, CV4 7AL, United Kingdom*

R. Osborn

*Rutherford Appleton Laboratory, Chilton, Didcot, Oxon., OX11 0QX, United Kingdom*

(Received 16 October 1991)

We report on a inelastic-neutron-scattering study of the crystal-field excitations in  $\text{Nd}_2\text{CuO}_4$  and  $\text{Pr}_2\text{CuO}_4$ , and in the related electron-doped, high-temperature superconductors  $\text{Nd}_{1.85}\text{Ce}_{0.15}\text{CuO}_4$ ,  $\text{Pr}_{1.85}\text{Ce}_{0.15}\text{CuO}_4$ , and  $\text{Nd}_2\text{CuO}_{3.7}\text{F}_{0.3}$ . The crystal-field splittings of the ground-state multiplet were studied in each of the compounds and supplementary information on the crystal field was obtained from intermultiplet excitations measured in the energy range 250–300 meV. We present a detailed theoretical analysis of the crystal field in the nonsuperconducting compounds. The calculations employ a spherical-tensor technique which allows for the mixing of the intermediate-coupling ground state with all excited  $J$  multiplets up to an energy of 2 eV. We have also incorporated a molecular-field term into the model to account for exchange interactions. We propose consistent crystal-field parameters for  $\text{Nd}_2\text{CuO}_4$  and  $\text{Pr}_2\text{CuO}_4$ , which achieve good agreement between the calculated and experimental transition energies, intensities, and magnetic susceptibilities. The excitation spectra of the superconducting compounds are found to exhibit some features in common, and we have deduced the presence of a molecular-field interaction with a magnitude of 0.10 meV in  $\text{Nd}_{1.85}\text{Ce}_{0.15}\text{CuO}_4$ .

### I. INTRODUCTION

The compounds  $L_2\text{CuO}_4$ , where  $L$  is one of the lanthanides Nd, Pr, or Sm, came into prominence several years ago when it was discovered that the substitution of Ce onto the  $L$  site, and subsequent annealing in a reducing atmosphere, could induce superconductivity.<sup>1,2</sup> Superconductivity can also be achieved for  $L = \text{Eu}$ ,<sup>3</sup> with Th doping instead of Ce in certain cases,<sup>3,4</sup> or with the substitution of a small amount of fluorine for oxygen.<sup>5</sup> Electronically, these superconductors differ in a significant way from the first cuprate superconductors to be discovered<sup>6</sup> which were based on  $\text{La}_2\text{CuO}_4$ . In the latter materials, a divalent dopant ( $\text{Sr}^{2+}$  or  $\text{Ba}^{2+}$ ) removes electrons from the Cu-O planes, leaving holes predominantly in the oxygen  $2p$  orbitals which are responsible for carrying the supercurrent. In contrast, the ability of cerium to exist in the tetravalent state, combined the observation of a negative Hall coefficient and thermoelectric power,<sup>2</sup> led to the suggestion that, in the newer materials, electrons are doped onto the planes, converting some of the  $\text{Cu}^{2+}$  ions into  $\text{Cu}^{1+}$ , and producing a superconductor with *negative* charge carriers. This possibility has serious implications for magnetic mechanisms of high-temperature superconductivity since  $\text{Cu}^{2+}$  carries a spin ( $S = \frac{1}{2}$ ) whereas  $\text{Cu}^{1+}$  does not. From a theoretical point of view, it is not clear whether a system with holes on some of the oxygen ions and a full complement of copper spins behaves in the same way as one with missing spins and extra electrons on some of the copper sites.

Apart from the sign of the charge carriers, the  $n$ -type family of superconductors and their parent compounds have other attributes which make them worthy of study.

In particular, these compounds have the simplest crystal structure of all the cuprate superconductors, with genuinely planar copper-oxide layers and no apical oxygen. Thus, in spite of their relatively low superconducting transition temperatures ( $T_c \approx 24$  K), the  $n$ -type superconductors are, in a sense, the most fundamental of all the high- $T_c$  superconductors, and the most theoretically tractable. These materials deserve a great deal of experimental effort to obtain detailed and reliable information on their microscopic properties.

Crystal-field spectroscopy is a sensitive probe of local electric and magnetic fields. This technique has been informative in the field of high- $T_c$  superconductivity, where it has been possible in certain materials to incorporate rare-earth ions carrying a magnetic moment into the structure in such a way that only a very weak interaction takes place with the electrons at the Fermi surface and the superconducting properties are hardly influenced by the substitution.<sup>7</sup>

Because superconductors are optically opaque at temperatures below  $T_c$ , neutron inelastic scattering is the appropriate technique to measure the crystal-field excitations. Neutron measurements of the crystal-field excitations in high- $T_c$  superconductors can be useful in several ways. The most obvious application is to obtain the interaction of the rare-earth ion with the crystal field. This is necessary for an understanding of the magnetic properties at low temperatures, such as the nature of the rare-earth magnetic ordering and the size of the ordered moment. Detailed measurements and analyses of the rare-earth-doped  $\text{YBa}_2\text{Cu}_3\text{O}_7$  series have now established a consistent model of the crystal field at the rare-earth site in this compound.<sup>8–10</sup> For the anomalous, nonsuperconducting compound  $\text{PrBa}_2\text{Cu}_3\text{O}_7$ , the observed crystal-

field spectrum has contributed strong evidence in support of the view that the Pr ions are trivalent but that they strongly interact with their environment.<sup>9–11</sup> A more unusual application of crystal-field measurements has been to study charge transfer during the hole- or electron-doping process as revealed by the changes in crystal-field spectra as a function of dopant concentration.<sup>12,13</sup> Finally, accurate measurements of the linewidths of crystal-field excitations in  $\text{Tm}_{0.1}\text{Y}_{0.9}\text{Ba}_2\text{Cu}_3\text{O}_7$  as a function of temperature have been used to study the energy gap and the spin susceptibility of the Cu-O planes.<sup>14</sup>

Encouraged by the development of a new generation of time-of-flight neutron spectrometers at pulsed spallation neutron sources, we undertook the present series of measurements with the aim of providing a thorough and reliable account of the crystal field in the *n*-type superconductors and parent materials. In particular, we have measured accurately the energies and the intensities of the crystal-field excitations and, because of the large incident energies available, we have also been able to observe excitations to the first excited *J* multiplets. These intermultiplet transitions can provide extra information in support of a model of the crystal field, and are particularly helpful with the light rare earths where the number of observable energy levels in the ground state is relatively small compared with the number of crystal-field parameters.

Neutron inelastic-scattering measurements of the crystal-field excitations in  $\text{Nd}_2\text{CuO}_4$  (Refs. 15–18) and  $\text{Pr}_2\text{CuO}_4$  (Refs. 19 and 20) have been reported by several groups, and preliminary accounts of our data for  $\text{Nd}_{1.85}\text{Ce}_{0.15}\text{CuO}_4$  and  $\text{Nd}_2\text{CuO}_{3.7}\text{F}_{0.3}$  have also been published.<sup>17,21</sup> With a view to a quantitative description of the crystal field in these compounds, we attempted initially<sup>17,21</sup> to analyze the results in the traditional way with Stevens' operators,<sup>22</sup> considering only transitions within the Hund's-rule ground-state multiplet. Others<sup>18,23</sup> have criticized this analysis, pointing out that, since the ground-state splittings in these compounds are of order 100 meV and the energy separation to the next *J* multiplet is about 250 meV for Nd and Pr, a significant admixture of the higher *J* states is expected. Alternative models were proposed by these authors for  $\text{Nd}_{2-x}\text{Ce}_x\text{CuO}_4$  and  $\text{Pr}_2\text{CuO}_4$  which included the lowest two multiplets in the crystal-field Hamiltonian.<sup>18,20,23</sup> These later calculations, while no doubt representing an improvement over the simplest analysis, should, in turn, be treated with some caution, since they themselves neglect a number of other corrections of similar magnitude.

Given the importance of the materials under investigation, and the success of the neutron experiments, we wished to undertake a more refined theoretical analysis that matched the statistical quality of the data. Our approach follows that described by Goodman and co-workers,<sup>24</sup> who have developed the basis for diagonalizing the full Hamiltonian for a rare-earth ion in a crystal-line environment in the intermediate-coupling scheme, including interactions between states in other *J* multiplets. We have added to this framework an extra interaction corresponding to the molecular field associated with

exchange interactions between the ions. As will be seen, not only do the values of the crystal-field parameters differ from those derived in previous calculations for  $\text{Nd}_2\text{CuO}_4$  and  $\text{Pr}_2\text{CuO}_4$ , but for the latter material we have also found it necessary to reconsider the ordering of the energy levels given previously.<sup>19,20</sup>

## II. EXPERIMENTS

Polycrystalline samples were used for all the neutron experiments. These were prepared in the standard way by a solid-state reaction of the appropriate starting materials:  $\text{Nd}_2\text{O}_3$  or  $\text{Pr}_6\text{O}_{11}$  and CuO for the parent materials, with the addition of  $\text{CeO}_2$  or  $\text{NdF}_3$  to make the superconductors. With the exception of the fluorinated compound, the materials were reacted at 950°C for between 2 and 10 days with intermittent regrindings. The powders were then pressed into cylindrical pellets of diameter 16 mm and thickness 3 mm, and sintered at around 1050–1100°C for the undoped, or 1100–1150°C for the doped materials, followed by an anneal in argon at 950–1000°C. For the fluorine-doped material, the reaction and sintering took place at a temperature of 900°C for a total time of 25 h, and the anneal was in nitrogen at the same temperature for 15 h. The samples were single phase to within the sensitivity of x-ray powder diffraction patterns, and superconductivity was observed in all the doped samples, with onset temperatures of around 21 K measured by ac susceptibility.

For the neutron measurements, the pellets were stacked together in an approximately square array with cadmium spacers separating each pellet, and with the cylinder axes perpendicular to the incident neutron beam. We have found that the use of cadmium to absorb neutrons scattered sideways between the pellets helps to reduce the level of the nonmagnetic (mainly Bragg + one-phonon) background in samples which are much broader than they are thick. The array of pellets was contained in an aluminum can which was mounted inside a pumped helium cryostat, capable of achieving a base temperature of 1.6 K. The total mass of sample in the neutron beam was between 50 and 100 g.

The neutron measurements were made on the high-energy transfer (HET) spectrometer at the spallation neutron source ISIS, part of the Rutherford Appleton Laboratory. HET is a direct-geometry, time-of-flight spectrometer<sup>25</sup> which uses a rotating Fermi chopper phased to the source proton pulse to select the incident neutron energy. The scattered neutrons are detected in two arrays of <sup>3</sup>He gas detectors situated at 4 and 2.5 m from the sample, and covering the angular ranges 3°–7° and 9°–29°, respectively. All the data presented in this paper were recorded in the 4-m detectors, for which the energy resolution is between 1.5 and 2.5% of the incident energy, depending on the energy transfer.

After subtraction of a time-independent background the spectra were converted from time-of-flight to energy transfer, and corrected for detector efficiency and for the  $k_f/k_i$  phase-space term in the cross section (see below). No attempt was made to put the scattering on an absolute scale as we are only interested in the relative intensities

ties of the crystal-field excitations. However, because in the time-of-flight method neutrons are recorded in detectors at fixed scattering angle, the scattering vector varies with energy transfer, so to compare intensities we corrected all spectra for the magnetic form factors of Nd<sup>3+</sup> or Pr<sup>3+</sup>.<sup>26,27</sup> To establish the integrated magnetic intensity under each peak, a good estimate of the non-magnetic background is required. This background is largely due to multiple scattering involving an elastic-scattering event and a one-phonon process, and therefore it reflects the phonon density of states.<sup>28</sup> Thus, a good indication of the structure in the background may be obtained from the spectrum measured at large angles (large Q), and with this as a guide it is possible to make a reasonable estimate of the integrated background under each peak. A single detector located at a scattering angle of 136° on HET may be used for this purpose. Nevertheless, it is the uncertainty in the background subtraction which contributes most to the uncertainty in the relative intensities of the excitations.

In order to characterize fully the excitations within the ground-state multiplet, various incident energies between 40 and 180 meV, and several temperatures between 1.6 and 200 K, were used. The intermultiplet transitions were measured at a temperature of 5 K, and with incident energies of 350, 500, and 600 meV.

### III. CRYSTAL-FIELD ANALYSIS

Until quite recently, neutron scatterers have only been able to study the crystal-field splitting of the ground-state multiplet of lanthanide ions in solids. In the analysis of the spectra it has in many cases been sufficient to treat the crystal-field interaction as a small perturbation on a pure Hund's-rule ground state, and to neglect the effects of intra-atomic interactions which were hitherto within the realm of optical spectroscopy. The new generation of neutron spectrometers has made it possible to measure the energies and transition probabilities of crystal-field excitations with high precision, and to observe transitions between different multiplets up to energies of more than 1 eV.<sup>29</sup> For a detailed interpretation of such spectra it is necessary to consider a more sophisticated atomic model. The programs used to analyze the data reported in this paper are based on those developed at Argonne and described in Refs. 9 and 10. We give a summary of the method here.

The atomic model is based on the assumption that the 4f<sup>n</sup> configuration of the lanthanide ion is well removed in energy from other electronic configurations, and the basis states are then one-electron wave functions calculated within the Hartree-Fock approximation. For the lanthanide ions the most important interaction is the Coulomb repulsion between the 4f electrons, which splits the 4f<sup>n</sup> configuration into Russell-Saunders terms diagonal in L and S, the combined orbital and spin angular momenta. The degeneracy of these states is further split by the spin-orbit interaction into states of well-defined J (the combined total angular momentum) but which are now of mixed L and S character. The resultant energy levels are relatively insensitive to the crystalline environment of the lanthanide ion, and the parameters of the

Coulomb and spin-orbit interaction may be obtained by fitting the model to optical data from ionic solids. In this study we have taken the free-ion parameters (including a number of others related to weaker interactions) from the work of Carnall *et al.*<sup>30</sup> on the spectra of lanthanides doped into LaF<sub>3</sub>.

Although these so-called "intermediate-coupling" wave functions are linear combinations of Russell-Saunders terms, it is found that the *ground states* of the lanthanide ions are dominated by a single term, the Hund's-rule ground state, which is often taken to be the pure ground state in elementary crystal-field theory. However, at the present level of analysis, we must consider the full intermediate-coupling ground state (and excited states also), which for the ion Pr<sup>3+</sup> is (in spectroscopic notation)

$$|^{2S+1}L_J\rangle_0 = 0.986|{}^3H_4\rangle + 0.166|{}^3F_4\rangle - 0.031|{}^1G_4\rangle$$

and for the ion Nd<sup>3+</sup> is

$$\begin{aligned} |^{2S+1}L_J\rangle_0 = & 0.984|{}^4I_{9/2}\rangle - 0.165|{}^2H_{9/2}^{(1)}\rangle \\ & + 0.057|{}^2H_{9/2}^{(2)}\rangle - 0.017|{}^2G_{9/2}^{(1)}\rangle \\ & + 0.015|{}^2G_{9/2}^{(2)}\rangle + 0.008|{}^4G_{9/2}\rangle \\ & + 0.003|{}^4F_{9/2}\rangle. \end{aligned}$$

Each of the intermediate-coupling wave functions is a multiplet of 2J + 1 degenerate states. In solids, these multiplets can be split by the crystalline electric field, and the extent to which the degeneracy is lifted depends upon J and upon the symmetry of the electric field. If the crystal-field splitting of the ground state is much smaller than the energy separation to the first excited multiplet, as is often the case with the heavier lanthanides, then it is a good approximation to diagonalize the crystal-field Hamiltonian within the basis of the ground-state J multiplet, and to neglect the existence of the excited states. However, as we shall see, the crystal-field splittings of the ground states of the compounds reported here are about 90 meV, and the first excited multiplets of Pr<sup>3+</sup> and Nd<sup>3+</sup> are typically 250 meV above the ground state, so the higher levels must be included in the diagonalization if we are to be consistent in the level of accuracy of the analysis. For the case of Pr<sup>3+</sup>, we chose to include all 13 J multiplets in the calculation, but for Nd<sup>3+</sup> the complete set of multiplets is too large to handle, so we included only the first 11 levels, extending 2.2 eV above the ground state.

The crystal-field Hamiltonian may be written in the form

$$H_{\text{CEF}} = \sum_{k,q} B_q^k C_q^k, \quad (1)$$

where C<sub>q</sub><sup>k</sup> is the qth component of a spherical tensor of rank k, and the B<sub>q</sub><sup>k</sup> are the corresponding crystal-field parameters. To a first approximation, the B<sub>q</sub><sup>k</sup> can be expressed as the product of two factors,

$$B_q^k = \langle r^k \rangle A_q^k, \quad (2)$$

of which the first is the kth moment of the 4f radial wave

function, and the  $A_q^k$  are intrinsic crystal-field parameters, independent of the particular lanthanide ion. Equation (2) provides a means of estimating the crystal-field parameters of different lanthanide ions doped into the same compound. We note that the crystal-field parameters defined by Eqs. (1) and (2) are sometimes confused with the symbols  $B_k^q$  used in the Stevens' operator formalism,<sup>22</sup> which is strictly valid only when  $H_{\text{CEF}}$  is diagonalized within the ground-state multiplet. The two sets of parameters are related by numerical scaling factors which have been tabulated.<sup>31</sup> The number of nonzero crystal-field parameters depends upon the point group of the lanthanide site, which, for the  $T'$ -phase structure of the present compounds, is  $D_{4h}$ . Accordingly, the crystal-field parameters are<sup>32</sup>  $B_0^2$ ,  $B_0^4$ ,  $B_0^6$ ,  $B_4^4$ , and  $B_4^6$ .

Up to this point the analysis has been concerned with electrostatic interactions with the crystalline environment of the lanthanide ion. There also exist weak magnetic interactions which must be taken into consideration if the low-temperature physical properties, such as the magnetic susceptibility and specific heat, are to be fully understood. These interactions have been incorporated into our model by the addition of a molecular-field (MF) term

$$H_{\text{MF}} = -\mu_B \hat{\mu} \cdot \mathbf{B}_{\text{MF}} \quad (3)$$

onto the Hamiltonian to represent the energy of the lanthanide ion in an effective molecular field,  $\mathbf{B}_{\text{MF}}$ , from the neighboring ions. In Eq. (3),  $\hat{\mu}$  is the magnetic moment operator in dimensionless units, and  $\mu_B$  is the Bohr magneton. The molecular-field term is relevant to the present investigation because of the existence of static magnetic order in the compounds. For instance, long-range antiferromagnetic order of the Nd moments has been observed by neutron diffraction in  $\text{Nd}_2\text{CuO}_4$  at about 4 K (Refs. 33–35) and in  $\text{Nd}_{1.85}\text{Ce}_{0.15}\text{CuO}_4$  at 1.2 K,<sup>36</sup> and the antiferromagnetic order of the Cu moments below 255 K has been shown<sup>37</sup> to induce a moment on the lanthanide ion proportional to the magnitude of the Cu moment in both  $\text{Nd}_2\text{CuO}_4$  and  $\text{Pr}_2\text{CuO}_4$ . In the magnetically ordered phases, the rare-earth and copper moments lie parallel to the tetragonal [110] direction. We assume that this is also the direction of the molecular field, and therefore rewrite Eq. (3) as

$$H_{\text{MF}} = -h_{\text{MF}}(\hat{\mu}_x + \hat{\mu}_y)/\sqrt{2}. \quad (4)$$

$h_{\text{MF}}$  as defined in Eq. (4) is a molecular-field parameter in energy units, but note that it differs from the equivalent parameter used in our previous paper<sup>17</sup> where  $h_{\text{MF}}$  was defined to include  $g_j$ , the Landé factor. With the molecular field perpendicular to the quantization axis, the crystal-field eigenvectors and matrix elements of the magnetic moment operator become complex. Care must then be taken to calculate the magnetic properties correctly.

In view of the size of the induced rare-earth moment and the low ordering temperature, the molecular-field interaction was expected to be much smaller than the crystal-field splitting, so it was treated by perturbation theory with terms included up to second order in  $h_{\text{MF}}$ . The perturbed eigenfunctions were then used to calculate

the transition probabilities, magnetic susceptibility and ordered moments.

The quantity measured by neutron inelastic scattering is the double-differential cross section (in  $\text{mb sr}^{-1} \text{meV}^{-1}$ ), given by<sup>38</sup>

$$\frac{d^2\sigma}{d\Omega d(\hbar\omega)} = 72.5 F^2(\mathbf{Q}) \exp(-2W) \frac{k_f}{k_i} S(\mathbf{Q}, \omega), \quad (5)$$

where  $\mathbf{Q}$  is the scattering vector,  $\hbar\omega$  is the energy transfer,  $F(\mathbf{Q})$  is the magnetic form factor,  $\exp(-2W)$  is the Debye-Waller factor (which we took to be unity in view of the small- $\mathbf{Q}$  values and low temperatures used in this experiment), and  $k_i$  and  $k_f$  are the magnitudes of the incident and scattered neutron wave vectors.  $S(\mathbf{Q}, \omega)$  is the response function, which is determined entirely by the temperature and the eigenfunctions of the system:

$$S(\mathbf{Q}, \omega) = \sum_{i,j} \rho_i |\langle j | \hat{\mu}_\perp | i \rangle|^2 \delta(E_i - E_j - \hbar\omega). \quad (6)$$

In Eq. (6),  $|i\rangle$  and  $|j\rangle$  are the initial and final eigenfunctions of the system corresponding to the eigenvalues  $E_i$  and  $E_j$ , respectively,  $\hat{\mu}_\perp$  is the component of the magnetic moment operator perpendicular to  $\mathbf{Q}$ , and  $\rho_i$  is the thermal population factor of the initial state.

To sum up the analysis procedure then, the Hamiltonian of the  $4f^n$  configuration is taken to be of the form

$$H = H_o + H_{\text{at}} + H_{\text{CEF}} + H_{\text{MF}}, \quad (7)$$

where  $H_o$  is the one-electron Hamiltonian,  $H_{\text{at}}$  accounts for intra-atomic interactions, mainly due to Coulomb repulsions and spin-orbit coupling,  $H_{\text{CEF}}$  is the crystal-field interaction, Eq. (1), and  $H_{\text{MF}}$  includes all exchange interactions via a molecular field, Eqs. (3) and (4). The molecular field was estimated from a number of different experimental quantities, as described below, and with the free-ion parameters treated as fixed constants the crystal-field parameters were adjusted by a weighted, least-squares-fitting procedure to achieve the best agreement between the calculated and observed transition energies and intensities. The crystal-field parameters derived in previous studies were used as starting parameters for the fit.

## IV. RESULTS

### A. $\text{Nd}_2\text{CuO}_4$ and $\text{Pr}_2\text{CuO}_4$

The crystal-field spectra of  $\text{Nd}_2\text{CuO}_4$  and  $\text{Pr}_2\text{CuO}_4$  measured by neutron scattering have been published on several occasions previously.<sup>15–20</sup> For reference, we show in Fig. 1 the low-energy excitations in  $\text{Nd}_2\text{CuO}_4$ , measured at a temperature of 1.6 K with neutrons of incident energy 40 meV, and in Figs. 2(a) and 2(b) the excitations in  $\text{Pr}_2\text{CuO}_4$  measured at 5 K with 250-meV neutrons, and at 150 K with 120-meV neutrons. We have described the excitations in  $\text{Nd}_2\text{CuO}_4$  previously,<sup>17</sup> and we simply list the observed transition energies and relative intensities in Table I.

Our measurements on  $\text{Pr}_2\text{CuO}_4$  are more revealing. As well as the strong ground-state transitions shown in Fig.

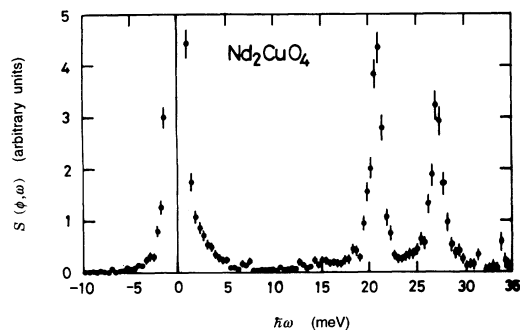


FIG. 1. Neutron-scattering spectrum of  $\text{Nd}_2\text{CuO}_4$  measured at a temperature of 1.6 K with neutrons of incident energy 40 meV at an average scattering angle,  $\phi$ , of  $5^\circ$ .

2(a) at 18 and 88 meV (the latter of which comprises two peaks, giving rise to the observed asymmetric line shape), several extra peaks appear in the 150 K spectrum clustered around 65 meV, and one at 73.5 meV, Fig. 2(b). These peaks correspond to transitions from the thermally populated 18-meV level to higher levels, some of which are not evident in the 5-K spectrum. For instance, the peak at 73.5 meV (which we have verified as magnetic from the reduction in intensity with  $|Q|$ , and have also observed in another run at 150 K with 150-meV incident neutrons) implies the existence of a crystal-field level at 91.5 meV situated above the highest level observed in Fig. 2(a) and connected to the ground state with a zero-transition matrix element. Such a level is not included in the scheme presented by Allenspach *et al.*<sup>20</sup> and caused

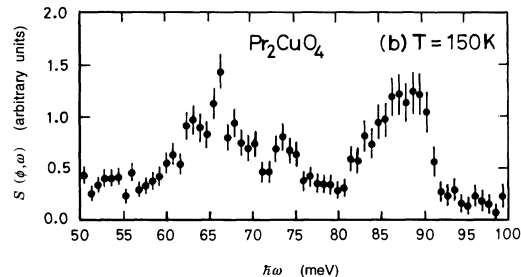
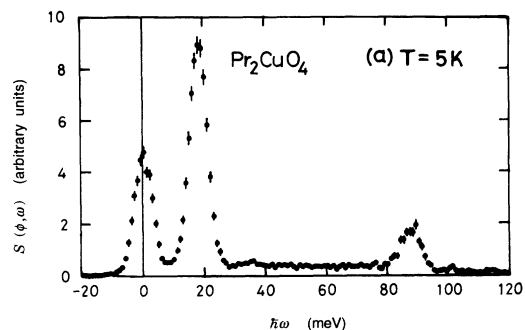


FIG. 2. Neutron-scattering spectrum of  $\text{Pr}_2\text{CuO}_4$  measured (a) at a temperature of 5 K and with the neutrons of incident energy of 250 meV, and (b) at 150 K and an incident energy of 120 meV. The neutrons were detected at an average scattering angle of  $5^\circ$ .

us to reconsider the order of the energy levels in the fit. The energies and relative intensities of all the excitations deduced from the spectra of  $\text{Pr}_2\text{CuO}_4$  are listed in Table II.

TABLE I. Observed and calculated crystal-field transitions within the ground-state multiplet of  $\text{Nd}_2\text{CuO}_4$ . The calculated relative intensities correspond to a temperature of 1.6 K, the same as used in the experiment. The levels joined by brackets are doublets not split by the crystal field.

Level $j$	$E_{\text{obs}}^a$ (meV)	$E_{\text{calc}}$ (meV)	$I_{\text{obs}}$ (Intensities relative to 21 meV level)	$I_{\text{calc}}$	Calculated transition probabilities, $ \langle j \hat{\mu}_\perp i\rangle ^2$	
					$i=0$	$i=1$
0	0.0	0.0			1.27	1.31
1	0.5 <sup>b</sup>	0.5			1.31	1.17
2	16±0.5 <sup>c</sup>	14.5	< 5	6	0.07	0.08
3		14.9			0.10	0.11
4	20.9±0.2	21.2	100	100	2.65	0.02
5		21.5			0.02	2.65
6	27.0±0.2	27.1	86±5	82	1.10	1.14
7		27.5			1.07	1.11
8	93.3±0.2	92.9	14±4	14	0.07	0.32
9		93.3			0.31	0.06

<sup>a</sup>Some of the energies have been revised slightly since the publication of Ref. 17 following more recent experiments.

<sup>b</sup>The splitting of the ground-state doublet by approximately 0.5 meV at low temperatures has been observed in a high-resolution, neutron experiment (Ref. 16).

<sup>c</sup>The existence of a doublet at around 16 meV was deduced from the presence of a peak at 11±0.5 meV in the spectrum measured at a temperature of 200 K.

TABLE II. Observed and calculated crystal-field transitions within the ground-state multiplet of  $\text{Pr}_2\text{CuO}_4$ . The calculated intensities correspond to a temperature of 5 K, the same as used in the experiment. The levels joined by brackets are doublets not split by the crystal field.

Level $j$	$E_{\text{obs}}$ (meV)	$E_{\text{calc}}$ (meV)	$I_{\text{obs}}$ (Intensities relative to 18 meV level)	$I_{\text{calc}}$	Calculated transition probabilities, $ \langle j \hat{\mu}_1 i\rangle ^2$		
					$i=0$	$i=1$	$i=2$
0	0.0	0.0			0.00	2.95	2.95
1]	18.1±0.2	18.1	100	100	2.95	0.00	1.88
2]		18.2			2.95	1.88	0.00
3		81.6			0.00	0.48	0.50
4]	84±1	84.4			0.18	1.06	0.00
5]		84.4	24±3	29	0.20	0.01	1.02
6	88±0.5	87.6			1.32	0.03	0.06
7		87.9			0.00	0.53	0.53
8	91.5±0.5 <sup>a</sup>	91.5			0.00	1.11	1.11

<sup>a</sup>Deduced from the presence of a peak at  $73.5\pm 0.5$  meV in the spectrum measured at a temperature of 150 K, Fig. 2(b).

The crystal-field parameters which gave the best description of the experimental data for  $\text{Nd}_2\text{CuO}_4$  and  $\text{Pr}_2\text{CuO}_4$  are presented in Table III. These parameters were used to obtain the calculated energies and intensities in Tables I and II. In Table II, we have also given the calculated transition probabilities to each level from the ground state and from the 18-meV doublet levels to demonstrate that the proposed level scheme is entirely consistent with the energies and relative intensities of the excited-state transitions observed in Fig. 2(b). For comparison, we list in Table III in the tensor operator notation the parameters given previously for  $\text{Nd}_2\text{CuO}_4$  by Boothroyd *et al.*,<sup>17</sup> Staub *et al.*,<sup>18</sup> and Nekvasil,<sup>23</sup> the parameters scaled from  $\text{Nd}^{3+}$  to  $\text{Pr}^{3+}$  according to the approximate factorization given by Eq. (2), and the parameters for  $\text{Pr}_2\text{CuO}_4$  according to Allenspach *et al.*<sup>20</sup> Considerable differences are seen between the earlier sets of parameters and the present results, and in view of the

sophistication of the present model we attribute these differences to the approximations made in the previous calculations. We note also that, within the present model, the parameters scaled from  $\text{Nd}^{3+}$  to  $\text{Pr}^{3+}$  are very close to the best-fit parameters for  $\text{Pr}^{3+}$  determined independently from the neutron data.

In Table III we have given a molecular-field parameter,  $h_{\text{MF}}$ , of 0.18 meV for  $\text{Nd}_2\text{CuO}_4$  since this raises the degeneracy of the ground-state doublet by 0.5 meV, as observed by neutron scattering,<sup>16</sup> and also because the Schottky specific-heat anomaly associated with such a splitting has a maximum at 2.3 K, in agreement with experiment.<sup>3</sup> We chose a molecular-field parameter of 0.16 meV for  $\text{Pr}_2\text{CuO}_4$  so as to give a saturated induced magnetic moment of  $0.08\mu_B$ , in accordance with that measured by neutron diffraction.<sup>37</sup> The ordered magnetic moment calculated for  $\text{Nd}^{3+}$  within our model is  $1.37\mu_B$ , which agrees well with the value of  $1.3\mu_B$  measured<sup>37</sup> at

TABLE III. Crystal-field parameters in tensor notation [Eq. (1)], and in units of meV, for  $L = \text{Nd}^{3+}$  and  $\text{Pr}^{3+}$  in  $L_2\text{CuO}_4$ , as determined in this investigation and in earlier studies.  $h_{\text{MF}}$  is a molecular-field parameter (also in meV), defined according to Eq. (4) to allow for an effective magnetic field at the lanthanide site in the [110] direction, and whose magnitude is fixed by experimental observation as described in the text.

Parameter	$\text{Nd}_2\text{CuO}_4$				$\text{Pr}_2\text{CuO}_4$		
	This work	Ref. 17	Ref. 18	Ref. 23	This work	Scaled from $\text{Nd}^{3+}$	Ref. 20
$B_0^2$	-28	-284	62	-64	-28	-30	-16
$B_0^4$	-263	-344	-241	-240	-301	-301	-251
$B_0^6$	34	-88	67	74	26	42	13
$B_4^4$	199	93	214	248	228	228	221
$B_4^6$	183	104	171	195	224	223	173
$h_{\text{MF}}$	0.18	0.43 <sup>a</sup>			0.16		0.14 <sup>b</sup>

<sup>a</sup>Note that, in Ref. 17,  $h_{\text{MF}}$  was defined so as to include the Landé factor. Here it has been converted to be consistent with the definition given in Eq. (4).

<sup>b</sup>This value is deduced from the molecular field of 2.5 T given in Ref. 20 via the relation  $h_{\text{MF}} = \mu_B B_{\text{MF}}$ .

0.6 K.

It is interesting to note that evidence for the molecular field can be observed in the ground-state excitation spectrum of  $\text{Nd}_2\text{CuO}_4$ , Fig. 1. An inspection of the 21- and 27-meV peaks will reveal that the latter is the broader which, as the calculated transition probabilities given in Table I show, is because in the 21-meV doublet only one component, 0 to 4, is connected to the ground state with measurable intensity, whereas for the 27-meV peak both the transitions 0 to 6 and 0 to 7 have approximately equal intensity. A further consequence of doublet splitting is that, if the sample is heated so as to populate both components of the ground-state doublet, then one expects the peak positions to shift to lower energies due to the emergence of transitions out of the upper level of the ground state. This effect is strikingly illustrated for  $\text{Nd}_2\text{CuO}_4$  in Fig. 3(a), where we have compared the 21- and 27-meV peaks at 1.6 and 50 K. The 27-meV peak is shifted down in energy by about 0.4 meV at the higher temperature as expected, but the 21-meV peak hardly shifts at all. We can understand why this is by considering again the transition probabilities given in Table I. The 21-meV peak only contains intensity from the transitions 0 to 4 and 1 to 5, which have almost the same energy separation, whereas the 27-meV peak is a weighted average of all four possible transitions between levels (0,1) and (6,7), so changes in position according to the relative thermal populations of levels 0 and 1. We also observe this effect for  $\text{Nd}_{1.85}\text{Ce}_{0.15}\text{CuO}_4$ , though to a lesser extent [Fig. 3(b)]. The molecular field does not cause a measurable splitting of the doublets in  $\text{Pr}_2\text{CuO}_4$ .

In some ways, it is not meaningful to attach an uncertainty to each of the crystal-field parameters because the five parameters are all correlated and so the variances

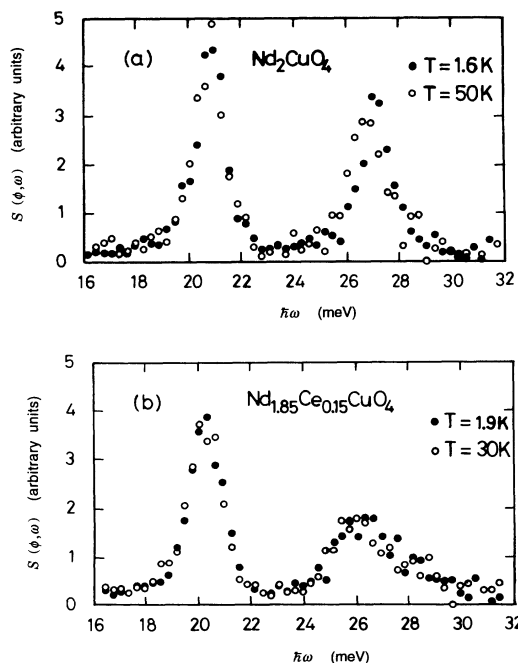


FIG. 3. Comparison of two of the crystal-field peaks at two different temperatures in (a)  $\text{Nd}_2\text{CuO}_4$ , and (b)  $\text{Nd}_{1.85}\text{Ce}_{0.15}\text{CuO}_4$ .

furnished by the fitting program are not independent. Nevertheless, one measure of the uncertainty is the spread in the values of the parameters obtained when slightly different sets of observables are supplied to the program. We have found that, for  $\text{Pr}_2\text{CuO}_4$ , the parameters in the “best-fit” set are defined on average to about 2 meV, in other words, other sets in which the parameters deviate by more than 2 meV predict energies and intensities which are not compatible with the accuracy of the experimental observables. For  $\text{Nd}_2\text{CuO}_4$ , on the other hand, the uncertainty is much larger, and different sets of parameters could be found with deviations of between 5 and 20 meV in the individual  $B$  coefficients which still give an adequate description of the neutron data. However, extra information on the crystal-field parameters can be extracted from the magnetic susceptibility. The anisotropy in the susceptibility is particularly sensitive to the value of  $B_0^2$ , and after comparison<sup>39</sup> of the predicted susceptibility with that measured<sup>39</sup> on a single crystal we were able to isolate the  $B_0^2$  coefficient, and hence the other four coefficients, in  $\text{Nd}_2\text{CuO}_4$  to within a few meV. The measured and calculated susceptibilities parallel,  $\chi_{\parallel}$ , and perpendicular,  $\chi_{\perp}$ , to the Cu-O planes are shown for  $\text{Nd}_2\text{CuO}_4$  and  $\text{Pr}_2\text{CuO}_4$  in Figs. 4(a) and 4(b).

The spectra described above represent the crystal-field splittings of the lowest  $J$  multiplets for  $\text{Nd}_2\text{CuO}_4$  and  $\text{Pr}_2\text{CuO}_4$ , and with both the transition energies and relative intensities there are a sufficient, if not overgenerous, number of observables to fit the five crystal-field parameters for these compounds. To provide an additional test

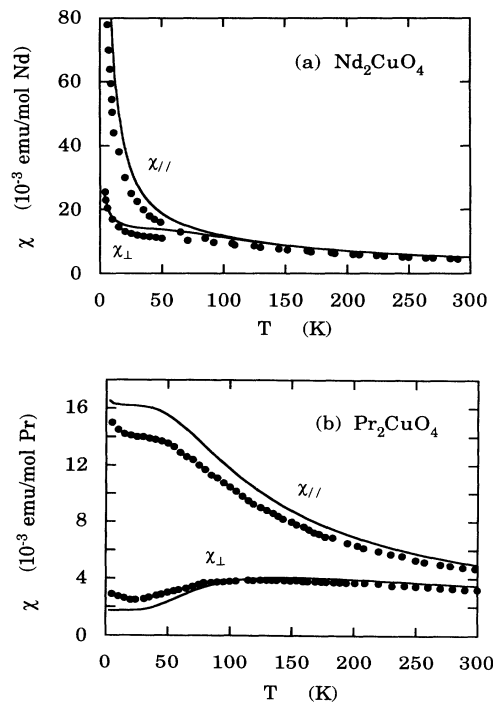


FIG. 4. Temperature dependence of the magnetic susceptibility measured parallel ( $\chi_{\parallel}$ ) and perpendicular ( $\chi_{\perp}$ ) to the Cu-O planes in (a)  $\text{Nd}_2\text{CuO}_4$  and (b)  $\text{Pr}_2\text{CuO}_4$ . The symbols are the measurements of Hundley *et al.* (Ref. 38), and the smooth curves are calculated from the crystal-field parameters given in Table III.

of the crystal-field model, we also measured the spectra at higher energies, where transitions from the ground state to levels within the first excited multiplet are expected. For  $\text{Nd}^{3+}$  this involves transitions from the predominantly  $^4I_{9/2}$  ground state to the  $^4I_{11/2}$  multiplet, and for  $\text{Pr}^{3+}$ , from the  $^3H_4$  to the  $^3H_5$  multiplet. In both cases, the intermultiplet excitations have  $\Delta J = 1$ ,  $\Delta S = \Delta L = 0$ , and are therefore magnetic dipole allowed and have a nonzero cross section at zero  $Q$ .

For the measurement of these intermultiplet transitions much higher incident neutron energies were required, and Fig. 5(a) and 5(b) show the spectra for  $\text{Nd}^{3+}$  and  $\text{Pr}^{3+}$  measured at 5 K with neutrons of incident energies 500 and 600 meV, respectively. The former shows clearly two peaks at 245 and 295 meV. The spectrum was actually measured on  $\text{Nd}_{1.85}\text{Ce}_{0.15}\text{CuO}_4$ , but was found to be identical to that of  $\text{Nd}_2\text{CuO}_4$  apart from being lower in energy by about 2 meV. For  $\text{Pr}_2\text{CuO}_4$ , only one peak was observed, centered on 290 meV, but its width is slightly larger than the energy resolution of the spectrometer at this incident energy, so could be comprised of several excitations close together. In Table IV we list for both compounds the energies and integrated neutron cross sections of the transitions from the ground state to the first excited state predicted by the model. The intermultiplet excitations are split into several groups by the crystal field, and the energies of the calculated transitions agree with the observed peaks to better than 1%. Although we have not corrected the spectra in Fig. 5(a) for the form factor of the intermultiplet transitions, the ratio of the two peak intensities in the spectrum of  $\text{Nd}_2\text{CuO}_4$  matches well with the calculated dipolar scattering cross sections (though at the  $Q$  values measured there may be appreciable nondipolar contributions to the intensity).

### B. The $n$ -type superconductors

Superficially, the neutron spectra obtained from the superconductors are very similar to those of the parent

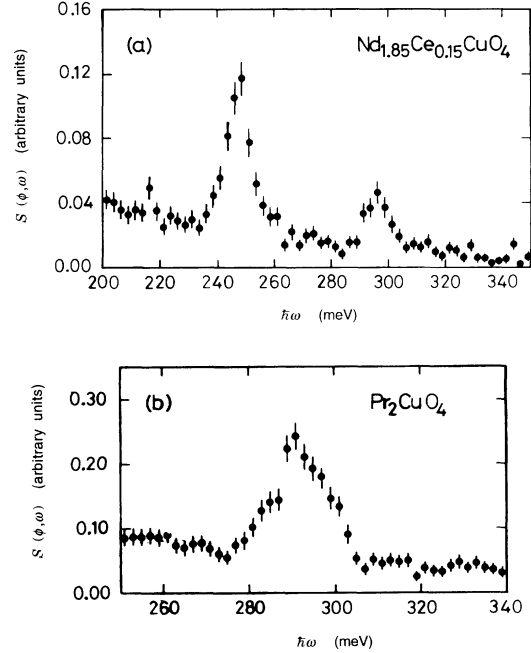


FIG. 5. Intermultiplet excitations measured at a temperature of 5 K at an average scattering angle of  $5^\circ$ . (a)  $\text{Nd}_{1.85}\text{Ce}_{0.15}\text{CuO}_4$ . Neutrons of incident energy 500 meV were used, and the two peaks correspond to excitations from the ground state of the  $^4I_{9/2}$  multiplet to levels within the first excited  $^4I_{11/2}$  multiplet which is split by the crystal field. (b)  $\text{Pr}_2\text{CuO}_4$ . Neutrons of incident energy 600 meV were used and the peak contains three excitations from the ground state  $^3H_4$  multiplet to the crystal-field-split  $^3H_5$  first excited multiplet.

compounds, as is to be expected given the rather small concentration of dopant. However, there are several features of the crystal-field transitions that the superconductors have in common, and that differentiate their spectra from that of  $\text{Nd}_2\text{CuO}_4$ . Figures 6(a) and 6(b) depict the low-energy part of the spectra of

TABLE IV. Intermultiplet transitions of  $L = \text{Nd}^{3+}$  and  $\text{Pr}^{3+}$  in  $L_2\text{CuO}_4$ . The calculated energies and integrated neutron cross sections were obtained from the parameters given in Table III and correspond to a temperature of 5 K. The observed energies represent the positions of the maxima of the measured peaks.

Level	$\text{Nd}_2\text{CuO}_4$			Level	$\text{Pr}_2\text{CuO}_4$		
	$E_{\text{obs}}$ (meV)	$E_{\text{calc}}$ (meV)	$\left[\frac{d\sigma}{d\Omega}\right]_{\text{calc}}$ (mb sr $^{-1}$ )		$E_{\text{obs}}$ (meV)	$E_{\text{calc}}$ (meV)	$\left[\frac{d\sigma}{d\Omega}\right]_{\text{calc}}$ (mb sr $^{-1}$ )
11	247 $\pm$ 2	247	54	10	292 $\pm$ 5	293	55
12		248	30	11		295	34
13		250	2	12		296	35
14		250	3	13		303	0
15		250	8	14		311	0
16		251	8	15		334	0
17		258	12	16		340	0
18		259	11	17		344	0
19	298 $\pm$ 2	297	21	18		345	0
20		298	7	19		346	1
21		300	5	20		346	1
22		300	4				



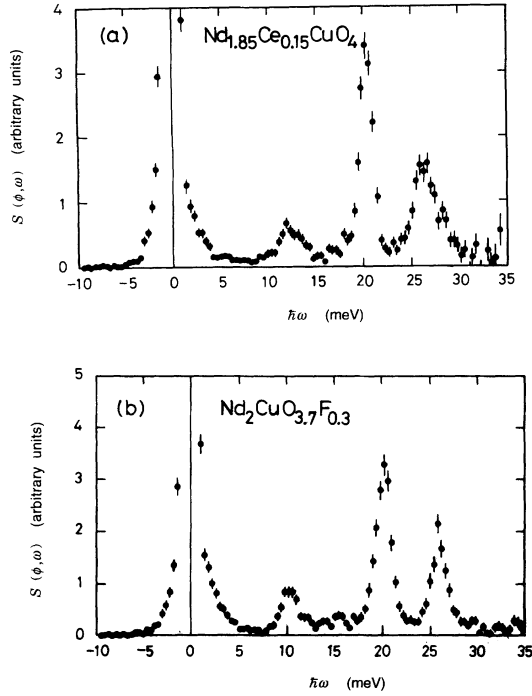


FIG. 6. Neutron-scattering spectrum of the superconducting compounds (a)  $\text{Nd}_{1.85}\text{Ce}_{0.15}\text{CuO}_4$  and (b)  $\text{Nd}_2\text{CuO}_{3.7}\text{F}_{0.3}$  measured at 2 K with neutrons of incident energy 40 meV at an average scattering angle of  $5^\circ$ .

$\text{Nd}_{1.85}\text{Ce}_{0.15}\text{CuO}_4$  and  $\text{Nd}_2\text{CuO}_{3.7}\text{F}_{0.3}$ , plotted on the same energy scale as Fig. 1 to facilitate a comparison with  $\text{Nd}_2\text{CuO}_4$ . The most immediate difference is that the lowest excited transition has gained considerable intensity compared with the equivalent excitation in

$\text{Nd}_2\text{CuO}_4$ , and has decreased in energy. In fact, all the peaks in Figs. 6(a) and 6(b) are lower in energy, and somewhat broader, than the corresponding ones in Fig. 1. Not shown in Fig. 6 are the 93-meV peaks, which for both superconductors appear distinctly split, with a second, slightly weaker component centered near 96 meV. In Table V we list the excitation energies (taken as the positions of the maxima of the main peaks) and relative intensities for the two Nd-containing superconductors.

With reference to our earlier discussion concerning the molecular field in  $\text{Nd}_2\text{CuO}_4$  and its influence on the neutron spectrum, we show in Fig. 3(b) the 20- and 26.5-meV peaks of  $\text{Nd}_{1.85}\text{Ce}_{0.15}\text{CuO}_4$  measured at temperatures of 2 and 30 K. By the same reasoning as before, the small reduction in energy of the 26.5-meV peak at the higher temperature implies the existence of a molecular field in superconducting  $\text{Nd}_{1.85}\text{Ce}_{0.15}\text{CuO}_4$  (and also in  $\text{Nd}_2\text{CuO}_{3.7}\text{F}_{0.3}$ , for which a similar effect was seen), whose magnitude is somewhat less than in  $\text{Nd}_2\text{CuO}_4$ . This possibility was proposed in our earlier work,<sup>17</sup> where we showed that, with a 0.28-meV splitting of the ground state, the calculated Schottky anomaly in the specific heat agreed very well with the peak observed in the experimental data. The implication here is that the  $\text{Nd}^{3+}$  ions experience an exchange interaction which is virtually independent of temperature at least up to 10 K, and which is no doubt responsible for the Nd antiferromagnetic order known<sup>36</sup> to occur below  $T_N \approx 1.2$  K. Our assertion that the specific-heat peak is almost entirely due to a Schottky anomaly and not, as previously suggested,<sup>3,36</sup> due to the magnetic transition is justified as long as the amount of entropy associated with the three-dimensional (3D) magnetic ordering at  $T_N$  is very small. This would be the case if the  $\text{Nd}^{3+}$  moments were strongly correlated in 2D above  $T_N$ . Since the moments in the copper sublatt-

TABLE V. Observed transition energies and relative intensities of the superconducting compounds  $\text{Nd}_{1.85}\text{Ce}_{0.15}\text{CuO}_4$  and  $\text{Nd}_2\text{CuO}_{3.7}\text{F}_{0.3}$  measured at a temperature of 2 K.

Level	$\text{Nd}_{1.85}\text{Ce}_{0.15}\text{CuO}_4$		$\text{Nd}_2\text{CuO}_{3.7}\text{F}_{0.3}$	
	$E_{\text{obs}}$ (meV)	$I_{\text{obs}}$ (Intensities relative to 20 meV level)	$E_{\text{obs}}$ (meV)	$I_{\text{obs}}$ (Intensities relative to 20 meV level)
0	0.0		0.0	
1				
2	$12.2 \pm 0.3$	$26 \pm 2$	$10.2 \pm 0.3$	$23 \pm 2$
3				
4	$20.3 \pm 0.1$	100	$20.2 \pm 0.3$	100
5				
6	$26.5 \pm 0.3$	$94 \pm 5$	$25.9 \pm 0.3$	$66 \pm 4$
7				
8	$93.2 \pm 0.5$	$24 \pm 2$	$93 \pm 1$	$14 \pm 4$
9				

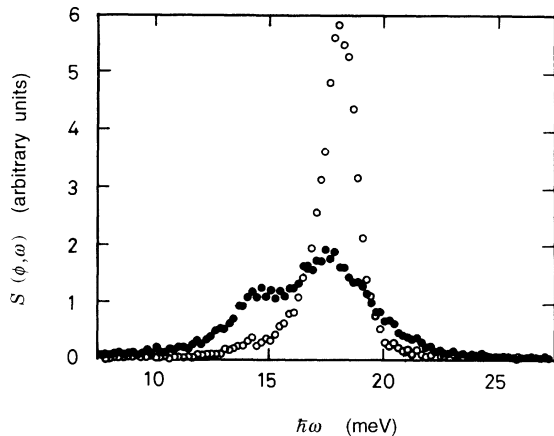


FIG. 7. The lowest-energy crystal-field transition of  $\text{Pr}_2\text{CuO}_4$  (open circles) and  $\text{Pr}_{1.85}\text{Ce}_{0.15}\text{CuO}_4$  (solid circles) measured at 5 K with neutrons of incident energy 60 meV. Two peaks can be resolved in the excitation of the superconductor.

tice do not order three dimensionality in the superconducting compounds, but are known to be strongly coupled in 2D, we suspect that the molecular field (and hence the 2D correlations of the  $\text{Nd}^{3+}$  moments) originates from regions of correlated Cu spins that are locally ordered in space and time. If we assume that the ground-state eigenvector for  $\text{Nd}_{1.85}\text{Ce}_{0.15}\text{CuO}_4$  is very similar to that for  $\text{Nd}_2\text{CuO}_4$ , then the molecular field required to achieve the aforementioned 0.28 meV splitting in the superconductor within the present model is  $h_{\text{MF}} = 0.10$  meV, about half that in  $\text{Nd}_2\text{CuO}_4$ .

The most notable difference between the spectra of  $\text{Pr}_{1.85}\text{Ce}_{0.15}\text{CuO}_4$  and  $\text{Pr}_2\text{CuO}_4$  is in the shape of the 18-meV peak, illustrated in Fig. 7 from runs with incident neutron energies of 60 meV. The former exhibits a multiple peak with two prominent components. The peak at 88 meV is also slightly broader in the superconductor, but no other significant differences were observed between the two spectra.

Our attempts to analyze quantitatively the data in Table V for  $\text{Nd}_{1.85}\text{Ce}_{0.15}\text{CuO}_4$  and  $\text{Nd}_2\text{CuO}_{3.7}\text{F}_{0.3}$  failed to achieve a description in terms of a single set of crystal-field parameters. Furrer *et al.*<sup>12</sup> have modeled the broadening of the crystal-field peaks in  $\text{Nd}_{1.85}\text{Ce}_{0.15}\text{CuO}_4$  in terms of two distinct  $\text{Nd}^{3+}$  environments, one of which is very similar to that found in  $\text{Nd}_2\text{CuO}_4$ , and the other which is a disturbed arrangement arising out of the local redistribution of negative charge from the Ce ions into the Cu-O planes. They proposed that the crystal field should be described by a combination of the five  $B$  coefficients derived for  $\text{Nd}_2\text{CuO}_4$ , together with another set of five for the  $\text{Nd}^{3+}$  ions in the “disturbed” environment. With the second set of parameters and a simple point-charge model, Furrer *et al.* found evidence for the transfer of electrons onto the Cu-O planes.

While we agree that the broadening of the excitations in the superconductors is likely to be caused by the existence of a number of subtly different  $\text{Nd}^{3+}$  environments, we do not accept that the two sets of parameters

given in Ref. 12 give an adequate description of the observed spectra, and therefore we suggest that the charge redistribution interpretation must be treated with some caution. The problem is, first, that the excitation energies of some of the transitions in the superconductors are lower by too much to justify retaining the  $\text{Nd}_2\text{CuO}_4$  parameters to describe the “undisturbed”  $\text{Nd}^{3+}$  site, and second, that the parameters found to describe the “disturbed” site cause a reduction in the ratio of the intensities of the 26.5- and 20-meV peaks, contrary to what is observed experimentally. A set of parameters has also been proposed<sup>40</sup> for  $\text{Nd}_{1.85}\text{Ce}_{0.15}\text{CuO}_4$  based on a fit to the anisotropic magnetic susceptibility measured on a single crystal. These parameters describe the susceptibility well within the model used, but fail to reproduce the intensity ratios of the measured transitions.

Accepting the model of two crystal-field environments for the superconductors, we attempted to find two sets of crystal-field parameters which together could provide a description of the spectra. The central task was to find sets of parameters which increased the intensity of the 12-meV peak relative to the 20 meV. Two distinct ways were found to achieve this objective, one of which caused a decrease in the intensity of the 26.5-meV peak to relative to the 20-meV peak, and the other which caused an increase in this ratio. Examples of the sets of parameters for these two cases, together with the corresponding crystal-field transitions, are given in Table VI. Of these, the first set are similar to those given in Ref. 12 with a positive  $B_0^2$  coefficient, while the second has  $B_0^2$  negative, as for  $\text{Nd}_2\text{CuO}_4$ , but larger in magnitude. Not surprisingly, the anisotropy in the susceptibility at high temperatures is in the opposite sense for these two possibilities, and we therefore looked towards experiment for gui-

TABLE VI. Examples of the two sets of crystal-field parameters and associated transitions which could correspond to different  $\text{Nd}^{3+}$  sites in the superconductors  $\text{Nd}_{1.85}\text{Ce}_{0.15}\text{CuO}_4$  and  $\text{Nd}_2\text{CuO}_{3.7}\text{F}_{0.3}$ . The full description of a magnetic property for the compound would be an average over that calculated with each set of parameters weighted according to the site occupancy.

Parameter set I (meV)		Parameter set II (meV)	
$B_0^2$	27	$B_0^2$	-80
$B_0^4$	-287	$B_0^4$	-231
$B_0^6$	60	$B_0^6$	64
$B_4^4$	220	$B_4^4$	237
$B_4^6$	175	$B_4^6$	174
$E_{\text{calc}}$ (meV)	$I_{\text{calc}}$ (Intensities relative to 20 meV level)	$E_{\text{calc}}$ (meV)	$I_{\text{calc}}$ (Intensities relative to 20 meV level)
0.0		0.0	
12.5	20	12.4	19
20.2	100	20.3	100
26.5	53	26.4	115
95.2	12	93.0	22

dance. The single-crystal measurements<sup>40</sup> revealed that the susceptibility of  $\text{Nd}_{1.85}\text{Ce}_{0.15}\text{CuO}_4$  is virtually identical to that of  $\text{Nd}_2\text{CuO}_4$ , and so if the present approach is to be viable, the two crystal-field environments would have to exist in roughly equal numbers. A similar approach is envisaged for  $\text{Nd}_2\text{CuO}_{3.7}\text{F}_{0.3}$ , but we do not have susceptibility data to check this.

On the surface, the above appears to provide a reasonable representation of the crystal-field excitations and magnetic susceptibility of  $\text{Nd}_{1.85}\text{Ce}_{0.15}\text{CuO}_4$ . However, we are rather skeptical as to its validity. For instance, it seems an unlikely coincidence that the susceptibilities of the  $\text{Nd}^{3+}$  ions in the two environments should combine together to yield a sum almost identical with the parent compound. Moreover, if we scale the  $\text{Nd}^{3+}$  parameters given in Table VI to  $\text{Pr}^{3+}$ , as was shown to work extremely well for the parent compounds, we calculate two very different crystal-field spectra, not at all consistent with that measured for  $\text{Pr}_{1.85}\text{Ce}_{0.15}\text{CuO}_4$ .

## V. CONCLUSIONS

In studying in detail the crystal-field excitations of  $\text{Nd}_2\text{CuO}_4$  and  $\text{Pr}_2\text{CuO}_4$  by neutron inelastic scattering, we have achieved what we believe is a reliable and accurate description of the crystal field in these compounds. This is essential if we are to understand what changes take place in the local electric and magnetic fields when a small concentration of *n*-type dopants is added to form superconductors. We emphasize the importance of including in the analysis not only the crystal-field energy levels but also the relative intensities of the peaks, which we have been able to determine with reasonable accuracy through the good resolution and low background characteristics of the HET spectrometer at ISIS.

To achieve the required analytic accuracy, we have used a rather advanced calculation that includes the intermediate-coupling wave functions and the admixture of higher *J* multiplets. This model has been successful in three ways: (i) the level of agreement attained between the measured and calculated neutron spectra is extremely good, (ii) the crystal-field parameters can be scaled in a simple way from  $\text{Nd}^{3+}$  to  $\text{Pr}^{3+}$  such that the scaled parameters are very close to the parameters obtained independently from the neutron spectra, and (iii) the crystal-field model derived from the splitting of the ground-state multiplet predicts the energies of the crystal-field-split, first excited multiplets to better than 1%. Thus, besides their importance in the field of high-temperature superconductivity, the compounds  $\text{Nd}_2\text{CuO}_4$  and  $\text{Pr}_2\text{CuO}_4$  have proved to be useful model systems for testing the accuracy of modern crystal-field calculations.

We have added an extra component to the crystal-field analysis by developing the formalism to include a molecular-field interaction in the model. With the direction of the molecular field parallel to [110], which is the same as the orientation of the Cu moments in the ordered phase, we have found the molecular field to be very simi-

lar in  $\text{Nd}_2\text{CuO}_4$  and  $\text{Pr}_2\text{CuO}_4$ . In the latter, the crystal-field ground state of the  $\text{Pr}^{3+}$  ion is nonmagnetic, so the molecular field strength is a measure of the Cu-Pr exchange interaction responsible for the small induced moment on the  $\text{Pr}^{3+}$  ion. The similar magnitude of the molecular field in  $\text{Nd}_2\text{CuO}_4$  suggests that it also arises largely from interactions between the lanthanide and copper ions, which indicates that the interaction responsible for the Nd ordering below 4 K is an indirect coupling of the Nd moments via the Cu-O planes. The same mechanism of exchange may be responsible for the Nd ordering observed in superconducting  $\text{Nd}_{1.85}\text{Ce}_{0.15}\text{CuO}_4$ , and we have deduced the presence of a molecular field in this compound about half as strong as in  $\text{Nd}_2\text{CuO}_4$ . The relevance of this molecular field to the superconductivity is not known, but its presence suggests that the 2D spin correlations of the Cu and Nd ions are related. A picture in which the molecular field arises from a local 2D ordering of the Cu spins with a slow spatial and temporal variation is consistent with the existence of a pseudogap in the spin excitation spectrum in the superconducting state, as has been proposed to explain other neutron-scattering results.<sup>14,41</sup>

The crystal-field spectra from the superconducting compounds exhibit two common features. First, the intensity of the lowest excitation is enhanced, and the energy depressed, for both of the  $\text{Nd}_2\text{CuO}_4$ -based superconductors. Second, the peaks are broader with the superconductors than with the parent compounds, which implies that several different local environments exist for the lanthanide ions. This effect is particularly noticeable for the lowest excitation of  $\text{Pr}_{1.85}\text{Ce}_{0.15}\text{CuO}_4$ , shown in Fig. 7. Although we have attempted to analyze the measurements in terms of two crystal-field environments, and have constructed a model that describes the neutron and magnetic data for  $\text{Nd}_{1.85}\text{Ce}_{0.15}\text{CuO}_4$ , the true picture is probably more complicated than this. A reliable model must be able to explain the changes that occur in the crystal-field spectra on doping to form a superconductor, the normal-state magnetic susceptibility and, we suspect, ought to employ a set of crystal-field parameters that are consistent with scaling from  $\text{Nd}^{3+}$  to  $\text{Pr}^{3+}$ . We believe that the present work has provided the basis for an understanding of the magnetic properties of the *n*-type superconductors, and hope that it will stimulate future investigations into the microscopic processes that lead to high- $T_c$  superconductivity.

## ACKNOWLEDGMENTS

We are indebted to G. L. Goodman for introducing us to the SHELL program which was originally developed by Crosswhite and Crosswhite, and which was modified by us to perform the present calculations. We would like to thank Zoë Bowden for her excellent technical support during the neutron experiments, and to acknowledge financial support from the Science and Engineering Research Council of Great Britain.

- \*Present address: Clarendon Laboratory, University of Oxford, Parks Road, Oxford, OX1 3PU, U.K.
- <sup>1</sup>Y. Tokura, H. Takagi, and S. Uchida, *Nature (London)* **337**, 345 (1989).
- <sup>2</sup>H. Takagi, S. Uchida, and Y. Tokura, *Phys. Rev. Lett.* **62**, 1197 (1989).
- <sup>3</sup>J. T. Markert, E. A. Early, T. Bjørnholm, S. Ghamaty, B. W. Lee, J. J. Neumeier, R. D. Price, C. L. Seaman, and M. B. Maple, *Physica C* **158**, 178 (1989).
- <sup>4</sup>J. T. Markert and M. B. Maple, *Solid State Commun.* **70**, 145 (1989).
- <sup>5</sup>A. C. W. P. James, S. M. Zahurak, and D. W. Murphy, *Nature (London)* **338**, 240 (1989).
- <sup>6</sup>J. G. Bednorz and K. A. Müller, *Z. Phys. B* **64**, 189 (1986).
- <sup>7</sup>J. M. Tarascon, W. R. McKinnon, L. H. Greene, G. W. Hull, and E. M. Vogel, *Phys. Rev. B* **36**, 226 (1987).
- <sup>8</sup>A. Furrer, P. Brüesch, and P. Unternährer, *Phys. Rev. B* **38**, 4616 (1988).
- <sup>9</sup>L. Soderholm, C.-K. Loong, G. L. Goodman, and B. D. Dabrowski, *Phys. Rev. B* **43**, 7923 (1991).
- <sup>10</sup>G. L. Goodman, C.-K. Loong, and L. Soderholm, *J. Phys. Condens. Matter* **3**, 49 (1991).
- <sup>11</sup>A. T. Boothroyd, L. W. Caves, D. M<sup>c</sup>K. Paul, and R. Osborn, *Bull. Mater. Sci.* **14**, 613 (1991).
- <sup>12</sup>A. Furrer, P. Allenspach, J. Mesot, and U. Staub, *Physica C* **168**, 609 (1990).
- <sup>13</sup>A. Furrer, P. Allenspach, J. Mesot, U. Staub, H. Blank, H. Mutka, C. Vettier, E. Kaldis, J. Karpinski, S. Rusiecki, and A. Mirmelstein, *Eur. J. Solid State Inorg. Chem.* **28**, 627 (1991).
- <sup>14</sup>R. Osborn and E. A. Goremychkin, *Physica C* **185-189**, 1179 (1991).
- <sup>15</sup>P. A. Alekseev, I. Yu. Arnold, S. E. Voinova, M. G. Zemlyanov, V. N. Lazukov, V. G. Orlov, P. P. Parshin, and I. P. Sadikov, *Superconductivity: Phys. Chem. Tech.* **2**, 163 (1989).
- <sup>16</sup>P. Hoffmann, M. Loewenhaupt, S. Horn, P. v. Aaken, and H.-D. Jostarndt, *Physica B* **163**, 271 (1990).
- <sup>17</sup>A. T. Boothroyd, S. M. Doyle, D. M<sup>c</sup>K. Paul, D. S. Misra, and R. Osborn, *Physica C* **165**, 17 (1990).
- <sup>18</sup>U. Staub, P. Allenspach, A. Furrer, H. R. Ott, S.-W. Cheong, and Z. Fisk, *Solid State Commun.* **75**, 431 (1990).
- <sup>19</sup>P. Allenspach, S.-W. Cheong, A. Dommann, P. Fischer, Z. Fisk, A. Furrer, H. R. Ott, and B. Rupp, *Z. Phys. B* **77**, 185 (1989).
- <sup>20</sup>P. Allenspach, A. Furrer, R. Osborn, and A. D. Taylor, *Z. Phys. B* **85**, 301 (1991).
- <sup>21</sup>A. T. Boothroyd, S. M. Doyle, D. M<sup>c</sup>K. Paul, D. S. Misra, and R. Osborn, *Bull. Mater. Sci.* **14**, 607 (1991).
- <sup>22</sup>K. W. H. Stevens, *Proc. Phys. Soc. London, Sect. A* **65**, 209 (1952).
- <sup>23</sup>V. Nekvasil, *Physica C* **170**, 469 (1990).
- <sup>24</sup>See L. Soderholm, C.-K. Loong, G. L. Goodman, and B. D. Dabrowski, *Phys. Rev. B* **43**, 7923 (1991), and references therein.
- <sup>25</sup>A. D. Taylor, B. C. Boland, Z. A. Bowden, and T. J. L. Jones (unpublished).
- <sup>26</sup>A. J. Freeman and J. P. Desclaux, *J. Magn. Magn. Mater.* **12**, 11 (1979).
- <sup>27</sup>E. J. Lisher and J. B. Forsyth, *Acta Crystallogr. A* **27**, 545 (1971).
- <sup>28</sup>R. Osborn (unpublished).
- <sup>29</sup>For a review of recent developments see R. Osborn, S. W. Lovesey, A. D. Taylor, and E. Balcar, in *Handbook on the Physics and Chemistry of the Rare Earths*, edited by K. A. Gschneidner, Jr. and L. Eyring (North-Holland, Amsterdam, 1991), Vol. 14, Chap. 93, p. 1.
- <sup>30</sup>W. T. Carnall, G. L. Goodman, K. Rajnak, and S. Rana, *J. Chem. Phys.* **90**, 3443 (1989).
- <sup>31</sup>A. J. Kassman, *J. Chem. Phys.* **53**, 4118 (1970).
- <sup>32</sup>U. Walter, *J. Phys. Chem. Solids* **45**, 401 (1984).
- <sup>33</sup>Y. Endoh, M. Matsuda, K. Yamada, K. Kakurai, Y. Hidaka, G. Shirane, and R. J. Birgeneau, *Phys. Rev. B* **40**, 7023 (1989).
- <sup>34</sup>S. Skanthakumar, H. Zhang, T. W. Clinton, W.-H. Li, J. W. Lynn, Z. Fisk, and S.-W. Cheong, *Physica C* **160**, 124 (1989).
- <sup>35</sup>M. J. Rosseinski, K. Prassides, and P. Day, *J. Chem. Soc. Chem. Commun.* **22**, 1734 (1989).
- <sup>36</sup>J. W. Lynn, I. W. Sumarlin, S. Skanthakumar, W.-H. Li, R. N. Skelton, J. L. Peng, Z. Fisk, and S.-W. Cheong, *Phys. Rev. B* **41**, 2569 (1990).
- <sup>37</sup>M. Matsuda, K. Yamada, K. Kakurai, H. Kadowaki, T. R. Thurston, Y. Endoh, Y. Hidaka, R. J. Birgeneau, M. A. Kastner, P. M. Gehring, A. H. Moudden, and G. Shirane, *Phys. Rev. B* **42**, 10098 (1990).
- <sup>38</sup>S. W. Lovesey, *Theory of Neutron Scattering from Condensed Matter* (Oxford University Press, Oxford, 1984), Vol. 2.
- <sup>39</sup>M. F. Hundley, J. D. Thompson, S.-W. Cheong, Z. Fisk, and S. B. Oseroff, *Physica C* **158**, 102 (1989).
- <sup>40</sup>G. Balakrishnan, S. K. Malik, C. K. Subramaniam, D. M<sup>c</sup>K. Paul, S. Pinol, and R. Vijayaraghavan, *J. Magn. Magn. Mater.* (to be published).
- <sup>41</sup>J. Rossat-Mignod, L. P. Regnault, C. Vettier, P. Burlet, J. Y. Henry, and G. Lapertot, *Physica B* **169**, 58 (1991).